PERGAMON

International Journal of Heat and Mass Transfer 42 (1999) 1147–1156

International Journal of HEAT and MASS TRANSFER

Technical Note
Turbulent heat transfer from a convex hemispherical surface to a round impinging jet

Dae Hee Lee*, Young Suk Chung, Moo Geun Kim

School of Mechanical and Automotive Engineering, Inje University, 607 Obang-Dong, Kimhae, Kyungnam 621-749, Korea

Received 20 June 1997; in final form 21 November 1997

Nomenclature

A surface area of the gold film Intrex
d pipe nozzle diameter
D outer diameter of the hemisphere
D/d hemisphere-to-nozzle diameter ratio
f gold coating uniformity factor
h heat transfer coefficient
I current across the gold film Intrex
k thermal conductivity of air
L/d dimensionless nozzle-to-surface distance
Nu local Nusselt number $[=hd/k]$
Nu_{st} stagnation point Nusselt number
q_c conduction heat loss
q_v net heat flux
r/d dimensionless streamwise distance from the stagnation point
Re Reynolds number based on the nozzle diameter $[=Ud/v]$
T_a ambient temperature
T_j jet temperature
T_w wall temperature of the convex surface
U mean velocity of air at the nozzle exit
V voltage across the gold film Intrex.

Greek symbols

ε emissivity of the liquid crystal and black paint coated surface (measured by infrared radiation thermometer: Minolta/5055)
v kinematic viscosity of air
σ Stefan–Boltzmann constant.

1. Introduction

As an effective method to enhance heat and mass transfer, impinging jets have been widely used in a variety of engineering applications such as cooling of hot steel plates, tempering of glass, drying of papers and textiles, cooling of turbine blades and electronic components, and manufacturing of TFT-LCD plate.

Numerous studies of the heat transfer and flow characteristics for the jet impingement on surfaces have been reported. These studies have dealt with the effects of Reynolds number, nozzle-to-surface distance, nozzle geometry, jet orientation, multiple jets, cross flow, and impinging surface shape on the resulting flow and heat transfer. Several review and summary papers on the impinging jet heat transfer have been published by Martin [1], Jambunathan et al. [2], and Viskanta [3]. Although many different jet characteristics have been considered, a great majority of impinging jet studies in the past were on the flat surface. However, many engineering applications of jet impingement cooling on curved surfaces may be encountered. A few papers have studied the impinging jet heat transfer from the curved surface. Chupp et al. [4] studied the heat transfer characteristics with an array of round jets impinging on a concave surface. Thomann [5] and Hrycak [6] reported the total heat transfer on the concave surface is higher than on the flat surface due to larger surface area especially for small nozzle-to-surface distances. For a highly concave surface, the optimum distance is less than for the equivalent flat surface case. With decreasing surface curvature and increasing nozzle-to-surface distance, the heat transfer characteristics approach those for the flat surface. Gau and Chung [7] investigatged the effects of surface curvature on the slot jet impingement heat transfer along semi-cylindrical concave and convex surfaces. They observed a series of three-dimensional counterrotating vortices near the stagnation point region on the convex surface. And they also found Taylor–Görtler vortices initiated along the concave surface. Yang et al. [8] investigated jet impingement cooling on the semi-cylindrical

* Corresponding author.

PII: S0017–9310(98)00174–4

concave surface with two different nozzles (round edged nozzle and rectangular edged nozzle).

In the present study, the local Nusselt numbers are measured for an air jet issuing from a long straight pipe and impinging perpendicular on the convex hemispherical surface. The experiments are made for $Re = 11\,000$–$87\,000$, $L/d = 2$–10, and $D/d = 10.6$. An electrically heated gold film Intrex (a very thin gold-coated polyester substrate sheet) is used to create a uniform heat flux on the convex surface. The temperature on the surface is measured using a thermochromic liquid crystal and a digital color image processing system.

2. Test apparatus and analysis

A schematic diagram of the test apparatus is shown in Fig. 1. The apparatus consists of a blower, a heat exchanger, an orifice flow meter, a long straight pipe with an inner diameter of $d = 2.87$ cm, and a convex hemispherical surface. The development length-to-diameter ratio of 51 results in a fully developed flow at the nozzle exit. A heat exchanger is used to maintain the jet temperature at the nozzle exit within $\pm 0.2^{\circ}$C of the ambient temperature. The test model consists of a 3.5 mm thick and 30.4 cm diameter Plexiglas convex hemisphere to which three 48 cm long strips (one 2.5 cm strip in the middle as a main heater and two 1.5 cm wide strips on both sides as guard heaters) of the gold film Intrex (a gold-coated polyester substrate sheet) are glued. An air brush is used to apply first the micro-encapsulated thermochromic liquid crystal and then black backing paint on the Intrex surface. A digital color image processing system is used to quantitatively determine the temperature corresponding to a particular color of liquid crystal. The measurement technique in this study, described by Lee et al. [9, 10], provides a method for determining the surface isotherms using liquid crystals. By electrically heating a very thin gold coating on the Intrex, an essentially uniform wall heat flux condition is established. The heat flux can be adjusted by changing the current through the Intrex, which changes the surface temperature. Under the constant heat flux condition, an isotherm on the Intrex surface corresponds to a contour of a constant heat transfer coefficient. The local heat transfer coefficient at the position of the particular color being observed is calculated from

$$h = q_v/(T_w - T_j) \tag{1}$$

where the net heat flux q_v is obtained by subtracting the heat losses from the total heat flux through the Intrex; i.e.

$$q_v = fIV/A - \varepsilon\sigma(T_w^4 - T_a^4) - q_c. \tag{2}$$

The ratio of the local electrical heating to the average heating, f, is a measure of the uniformity of the gold coating on the Intrex. Baughn et al. [11] found the uniformity to be as high as 98% when the test section of the Intrex is small and selected from the middle of a roll where the gold-coating is most uniform, which has been the case for the present experiment. Therefore, we assume $f \approx 1$ for the heat flux calculation, but f is maintained in equation (2) because it contributes to the overall Nusselt

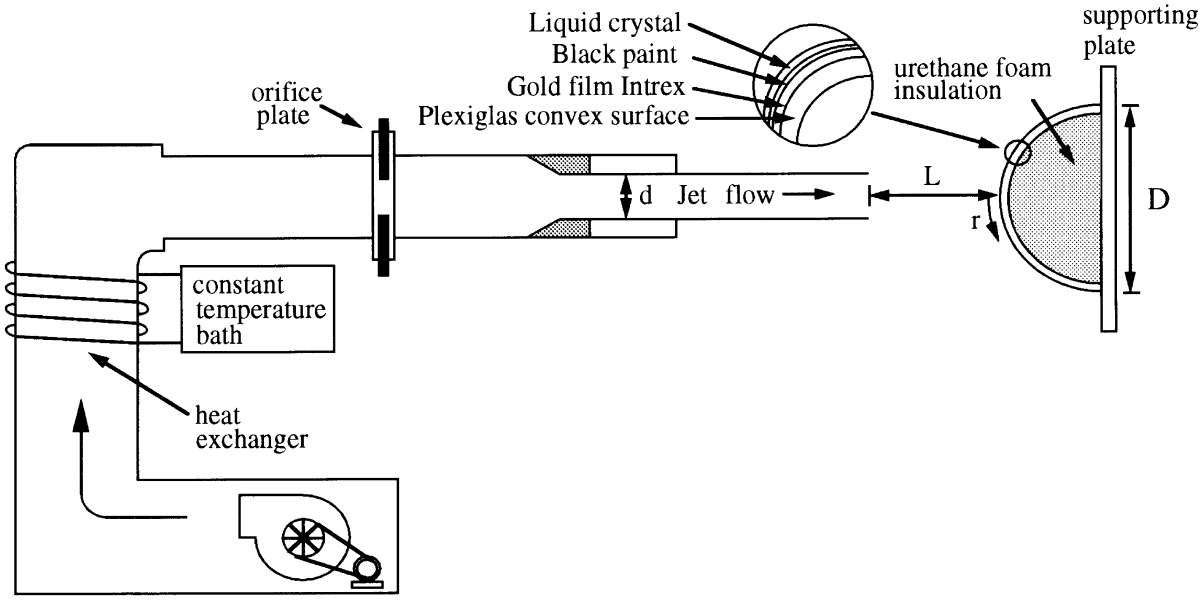

Fig. 1. Schematic diagram of the test apparatus for the jet impingement on the convex hemispherical surface.

Table 1
Nusselt number uncertainty analysis

x_i	Value	δx_i	$\left(\frac{\delta x_i}{Nu}\frac{\partial Nu}{\partial x_i}\right)\times 100\,(\%)$
f	1.0	0.02	2.62
ε	0.9	0.05	2.0
q_c	0 (W/m^2)	4.58	1.26
T_w	35.69 (°C)	0.20	1.15
T_j	12.97 (°C)	0.15	0.86
A	0.16 (m^2)	8.3×10^{-5}	0.66
I	0.183 (A)	7.77×10^{-4}	0.56
V	41.6 (V)	0.125	0.39
d	28.7 (mm)	0.05	0.21

Total Nu uncertainty: d$Nu/Nu = 3.95\%$

number uncertainty (Table 1). The conduction loss, q_c, through the back of the plate is small compared to the surface heating and is assumed to be zero. However, it is included in the equation because it also contributed to the overall Nusselt number uncertainty.

The uncertainty analysis has been carried out using the method by Kline and McKlintock [12]. Table 1 shows that the Nusselt number uncertainty for $L/d = 10$ and $r/d = 6.1$ at $Re = 11\,000$ is 3.95%. It should be noted that this uncertainty represents the maximum uncertainty in the Nusselt number under the given experimental conditions. The uncertainty in the gold coating uniformity is the largest contribution to the overall Nusselt number uncertainty. Another important source of uncertainty is the emissivity of liquid crystal and black paint. The present uncertainty estimates are based on 20 : 1 odds (i.e. 95% confidence level of both the precision and bias errors).

3. Results and discussion

The stagnating point Nusselt number (Nu_{st}) vs. the dimensionless nozzle-to-surface distance (L/d) is plotted in Fig. 2 for various jet Reynolds numbers. It can be seen from Fig. 2 that for $L/d < 4$, there is essentially no variation of Nu_{st} with L/d. For $L/d \geqslant 4$, Nu_{st} gradually increases with L/d and reaches a maximum at $L/d = 6$ for $Re = 11\,000$ and 23 000, and at $L/d = 8$ for $Re \geqslant 50\,000$, respectively. A downstream shift of the maximum Nu_{st} position from $L/d = 6$ to $L/d = 8$ is attributed to an increase of the potential core length with increasing Reynolds number. This agrees well with the results of Lee et al. [9], Yan [13], and Kataoka et al. [14] for a round jet impinging upon the flat surface for $10\,000 \leqslant Re \leqslant 50\,000$. Lee et al. [9] and Kataoka et al. [14] showed that the physical mechanism for the maximum Nu_{st} to occur at $L/d = 6$–8 is that a change in the jet centerline velocity from the initial centerline velocity is not only small, but the turbulent intensity reaches roughly a maximum value in that region.

Correlations of Nu_{st} in terms of the Reynolds number and the nozzle-to-surface distance are plotted in Figs 3 and 4 and obtained as follows:

For $2 \leqslant L/d < 8$, $Nu_{st} = 1.14(Re)^{0.48}(L/d)^{0.09}$ with a scatter of 0.6%.

For $8 \leqslant L/d \leqslant 10$, $Nu_{st} = 1.14(Re)^{0.54}(L/d)^{-0.55}$ with a scatter of 0.1%.

It should be noted that for $2 \leqslant L/d < 8$, Nu_{st} varies according to $Nu_{st} \propto Re^{0.48}$, which approximately agrees with the $Re^{0.5}$ laminar boundary layer flow result. For the longer distances, the Reynolds number dependence is stronger ($Nu_{st} \propto Re^{0.54}$ for $8 \leqslant L/d \leqslant 10$). This may be due to an increase of turbulence in the approaching jet as a result of the stronger exchange of momentum with the ambient air. Gau and Chung [7] also show that $Nu_{st} \propto Re^{0.5}$ for $2 \leqslant Z/b < 8$ and $Nu_{st} \propto Re^{0.54}$ for $8 \leqslant Z/b \leqslant 16$ (where Z/b is the dimensionless nozzle-to-surface distance). It is also observed that Nu_{st} is nearly independent of L/d for $2 \leqslant L/d < 8$, but varies according to $Nu_{st} \propto (L/d)^{-0.55}$ for $8 \leqslant L/d \leqslant 10$, which is consistent with the fluid mechanics results by Lee et al. [15].

Figures 5 and 6 show comparisons of Nu_{st} and the streamwise local Nusselt number distributions between the convex and flat surfaces for $L/d = 4$, respectively. The values of Nu_{st} for the convex surface are approximately 6–12% higher than those for the flat surface for the Reynolds numbers tested. According to our flow visualization test by smoke wire, higher values of Nu_{st} for the convex surface case is attributed to a series of three-dimensional counterrotating vortices initiated near the wall at the stagnation point region, which cause an increase of momentum transport in the flow and subsequent enhancement of the heat transfer rate. It is also observed from Fig. 6 that these vortices persist even in the wall jet region and the Nusselt number values in that region for the convex surface are higher than those for the flat surface. Gau and Chung [7] also report a similar behaviour in their research that investigated the effect of a surface curvature on slot air jet impingement heat transfer along convex surfaces.

The streamwise Nusselt number distributions divided by Re^n are presented in Figs 7–9 for three nozzle-to-surface distances of $L/d = 2$, 6, and 8, five jet Reynolds numbers ranging from 11 000 to 87 000. These results show that there is a two-region feature concerning the Reynolds number dependence. For $L/d = 2$, the Nusselt number distributions in the region corresponding to $r/d < 1.5$ are well correlated with a Reynolds number power of $n = 0.45$, indicating that the flow in the stagnation point region is laminar. On the other hand, the Nusselt number distributions in the wall jet region corresponding to $r/d \geqslant 2.0$ are also well correlated with a

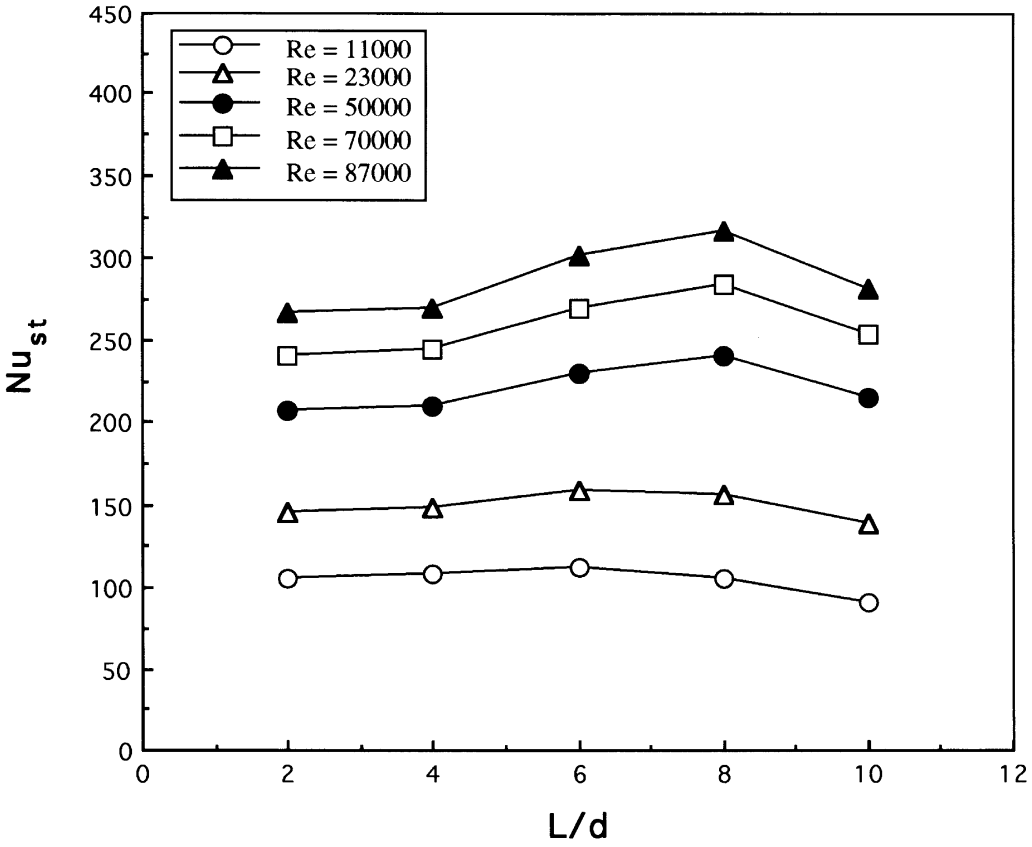

Fig. 2. Effect of the nozzle-to-surface distance on the stagnation point Nusselt number for different jet Reynolds numbers.

Reynolds number power of $n = 0.65$, suggesting that the wall jet flow has a turbulent boundary layer. For longer nozzle-to-surface distances of $L/d = 6$ and 8, the Reynolds number dependence for $r/d \geqslant 2.0$ shows $n = 0.67$ for both cases. But, for $r/d < 1.5$, there appears to be a stronger Reynolds number dependence ($n = 0.48$ for $L/d = 6$ and 0.53 for $L/d = 8$) than for the shorter nozzle-to-surface distance of $L/d = 2$. This is due to the fact that for $L/d > 4$, the impinging surface is positioned outside of the potential core of the jet and a subsequent increase of the entrainment of the surrounding air to the jet flow has affected the heat transfer rate at the stagnation point region.

Similar results were reported by Yan [13] and Hollworth and Gero [16] in their studies with the flat surface. Yan [13] reported $n = 0.5$ in the stagnation region for $L/d = 2$ and 4, and $n = 0.56$ for $L/d = 6$ and $n = 0.58$ for $L/d = 10$; in the wall jet region $n = 0.7$ for all L/d. Hollworth and Gero [16] studied the heat transfer for the jet issuing from a square-edged orifice for Reynolds numbers from 5000 to 60 000. Their results show $n = 0.65$, 0.76, 0.79, and 0.8 at $r/d = 0$, 3, 6, and 9, respectively for one nozzle-to-plate distance, $L/d = 5$. There appears to be some discrepancies in the exponent between these results. This may be attributed to differences in the experimental conditions such as nozzle geometry, turbulence intensity level, shape of the impinging surface, jet temperature and etc.

Figures 7–9 show that the local Nusselt number decreases from its maximum value at the stagnation point as the thermal boundary layer thickness grows with r/d. However, for $L/d = 2$, the local Nusselt number distributions exhibit increasing values at $r/d \cong 1.2$–1.5 and attain secondary maxima at $r/d \cong 2.2$. An occurrence of the secondary maxima in the Nusselt number is attributed to the fact that because the impinging surface is within the potential core region, the potential core of the jet flow impinges upon the surface so that initially the laminar boundary layer develops from the stagnation point and a transition process takes place until the flow becomes turbulent at $r/d \cong 2.2$, resulting in a sudden increase in the heat transfer rate. Secondary maxima have also been reported in the flat surface study by Yan [13] and in the convex surface study by Gau and Chung [7] at $r/d \cong 2$ for $L/d = 2$ and $23\,000 \leqslant Re \leqslant 70\,000$, and $r/b \cong 7$ for $Z/b = 4$ and $Re = 11\,000$, respectively.

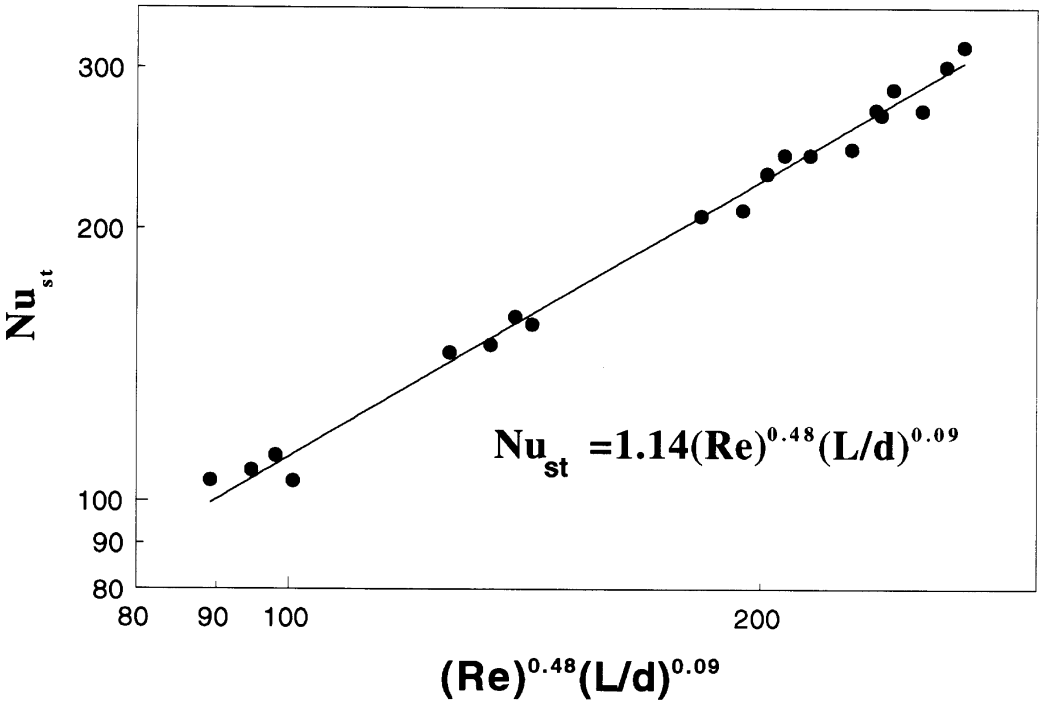

Fig. 3. Correlation of the stagnation point Nusselt number on the convex surface for $2 \leqslant L/d < 8$.

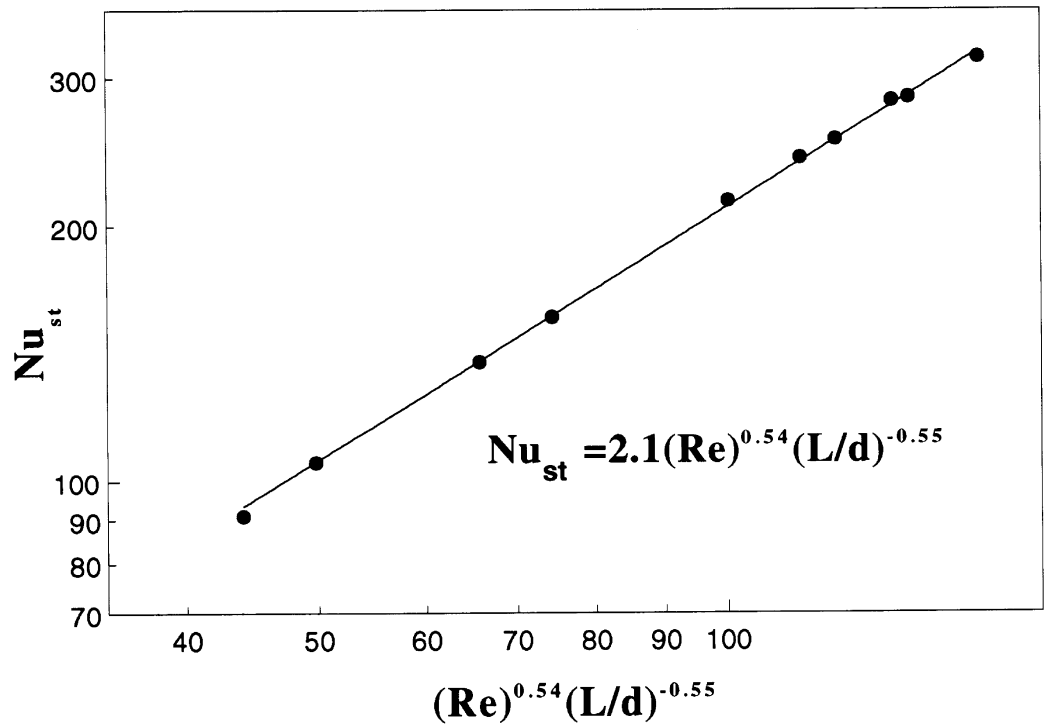

Fig. 4. Correlation of the stagnation point Nusselt number on the convex surface for $8 \leqslant L/d \leqslant 10$.

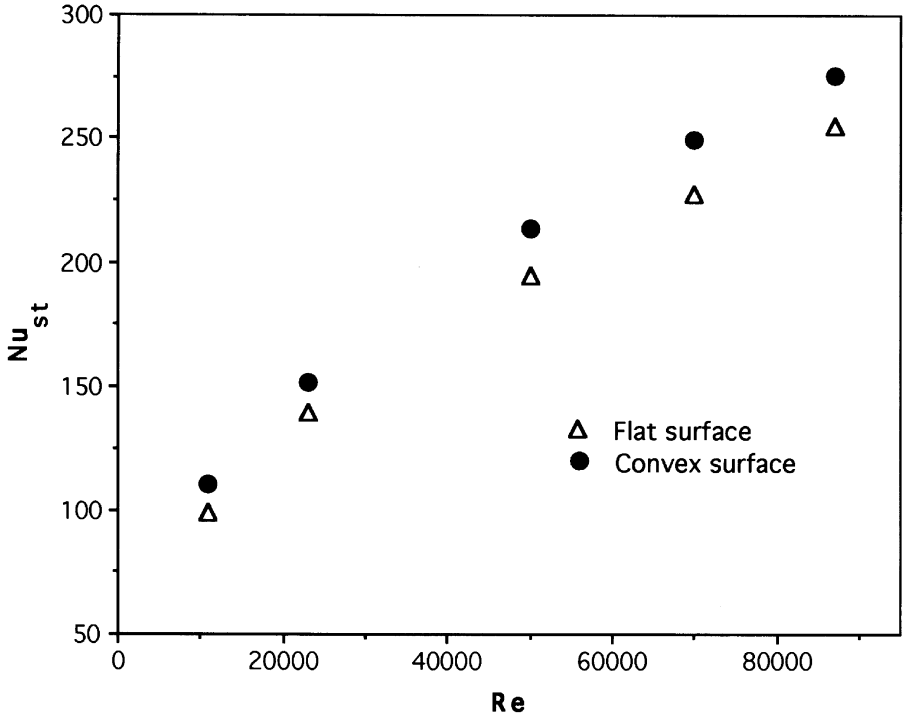

Fig. 5. Comparison of the stagnating point Nusselt number between the convex and the flat surfaces for $L/d = 4$.

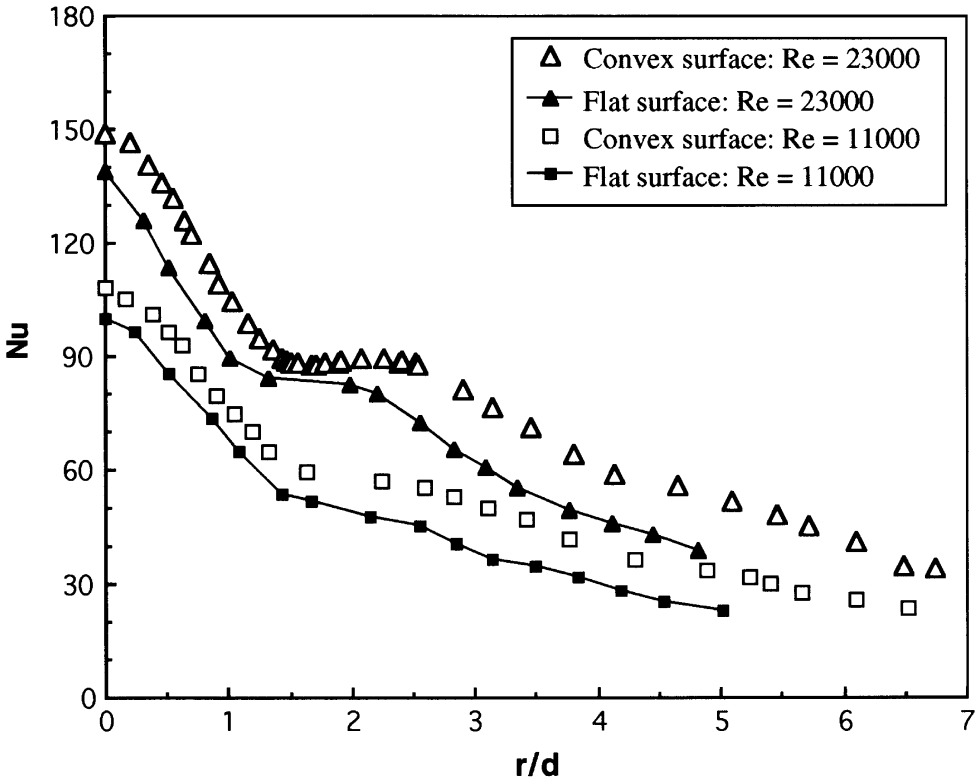

Fig. 6. Comparison of the Nusselt number distributions between the convex and flat surfaces for $L/d = 4$.

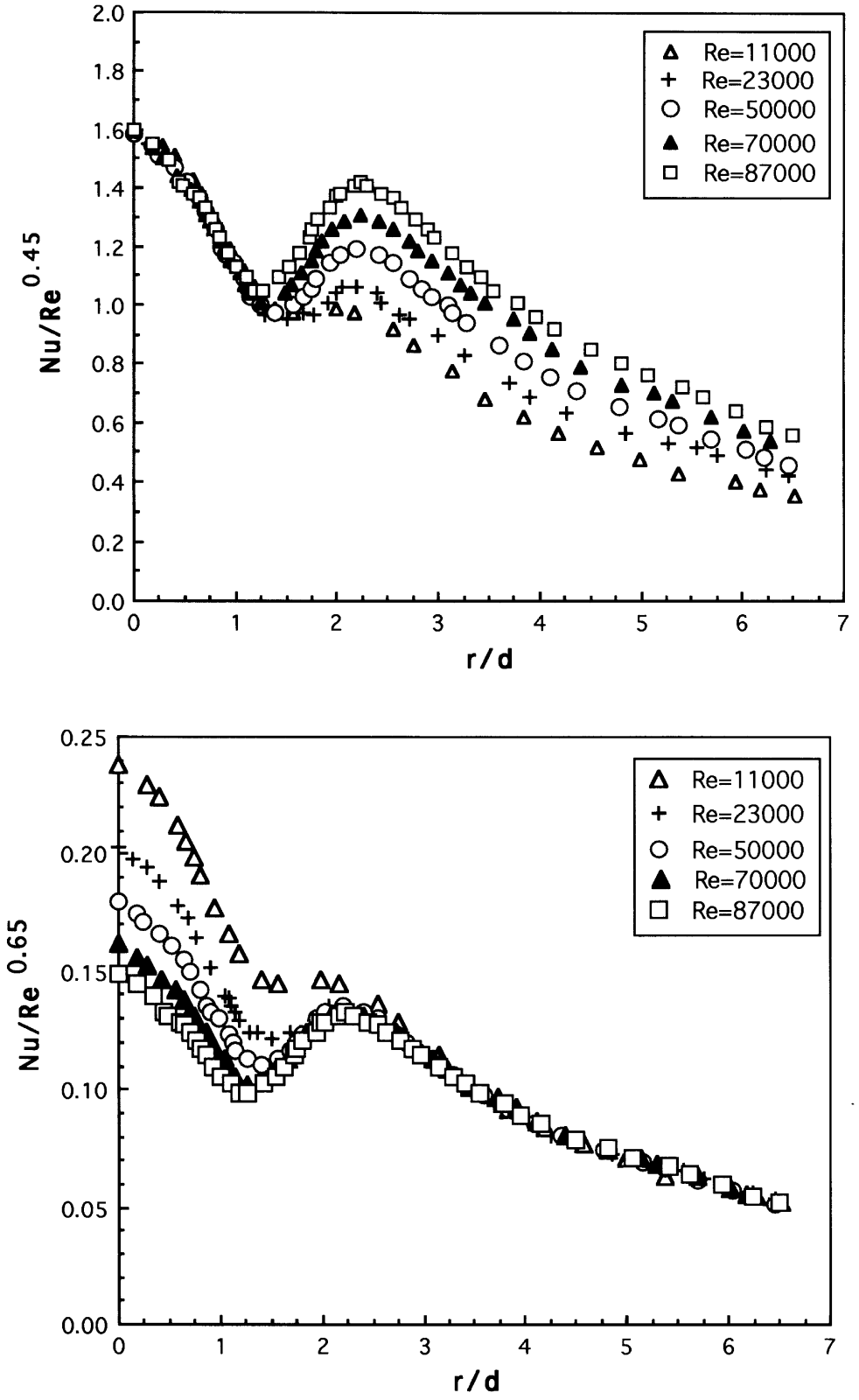

Fig. 7. Dependence of the streamwise Nusselt number upon Reynolds number for $L/d = 2$.

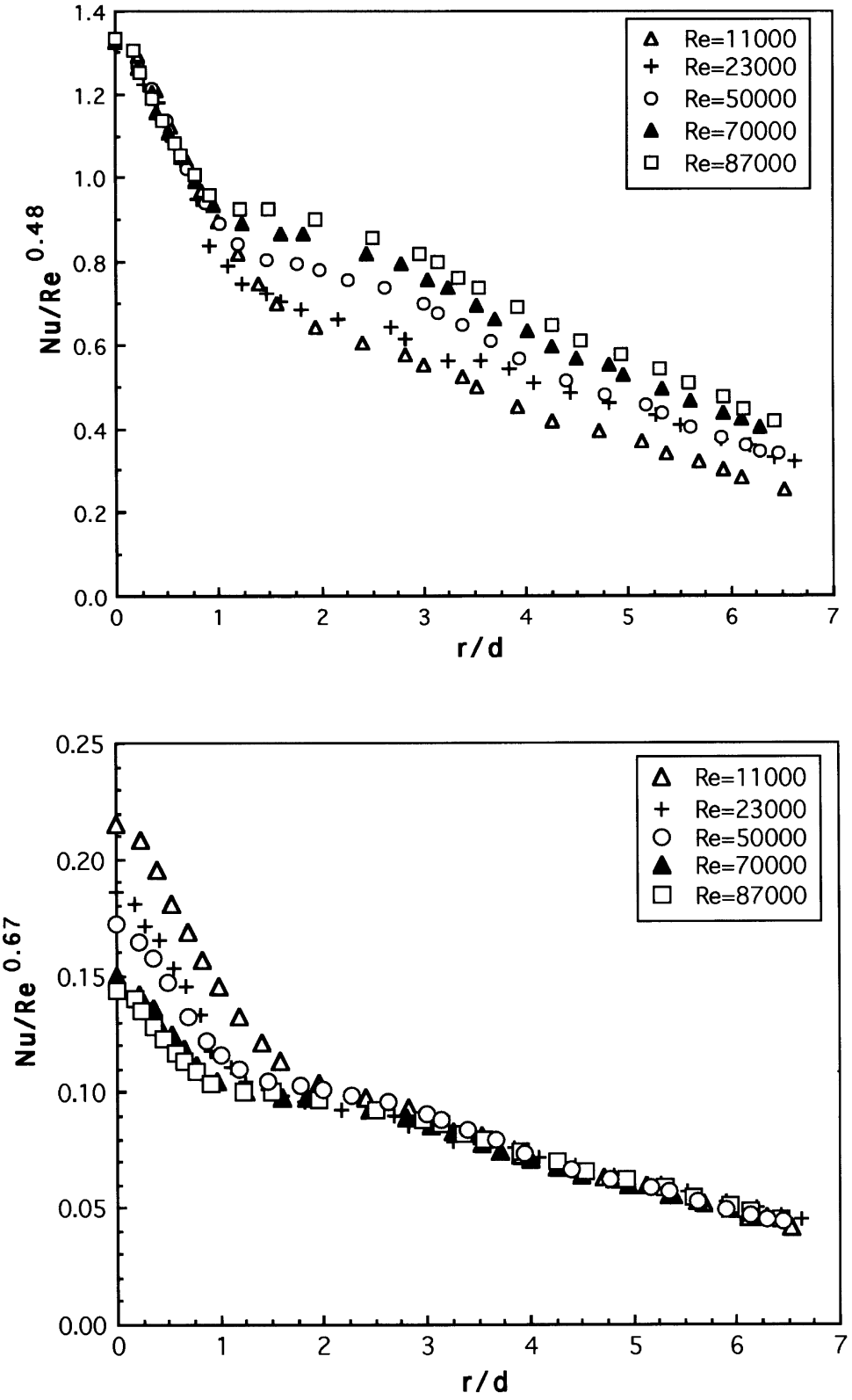

Fig. 8. Dependence of the streamwise Nusselt number upon Reynolds number for $L/d = 6$.

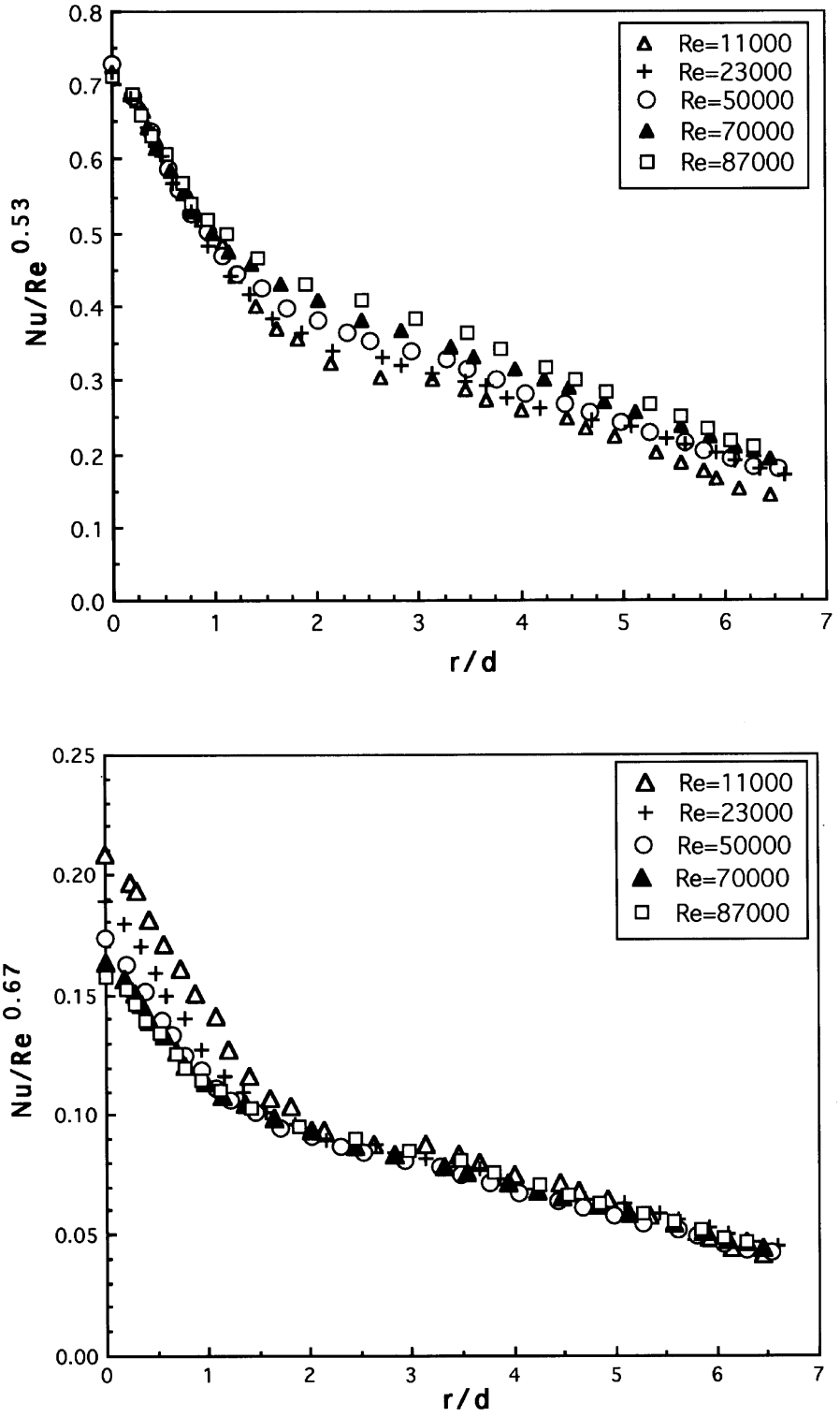

Fig. 9. Dependence of the streamwise Nusselt number upon Reynolds number for $L/d = 8$.

When the impinging surface is positioned outside of the potential core region (i.e. $L/d > 4$), a turbulence level in the jet flow approaching the surface is becoming high due to an increased entrainment of surrounding air to the jet flow. Therefore, a higher Nusselt number at the stagnation point and a monotonic decrease of the local Nusselt number in the downstream region can be expected as shown in Figs 8 and 9.

4. Conclusions

The experimental study has been carried out to investigate the effects of the Reynolds number and the nozzle-to-surface distance on the heat transfer from a hemispherically convex surface to a round impinging jet. For $L/d \geqslant 6$ and all Reynolds numbers, the local Nusselt number decreases monotonically from its maximum value at the stagnation point. However, for $L/d = 2$, the local Nusselt number distributions exhibit increasing values in the region $1.2 \leqslant r/d \leqslant 1.5$ and attain secondary maxima at $r/d = 2.2$. The formation of the secondary maxima is attributed to an increase in the turbulence level resulting from the transition from a laminar to a turbulent boundary layer.

The maximum Nusselt number at the stagnating point occurs at $L/d \cong 6$ for $Re = 11\,000$ and $23\,000$, and $L/d \cong 8$ for $Re \geqslant 50\,000$, which implies a longer potential core length for higher Reynolds number. The stagnation point Nusselt number (Nu_{st}) is well correlated with Re and L/d. For larger L/d, Nu_{st} dependence on Re is stronger due to an increase of turbulence in the approaching jet as a result of the stronger exchange of momentum with the surrounding air.

The Nusselt number values for the convex surface are higher than those for the flat surface. This may be attributed to a series of three-dimensional counterrotating vortices initiated on the convex wall. These vortices can increase momentum transport in the flow and enhance the heat transfer rate. Plots of Nu/Re^n versus r/d show that there is a two-region feature concerning the Reynolds number dependence ($n = 0.45$–0.53 in the stagnation region and $n = 0.65$–0.67 in the wall jet region). This change of the Reynolds number power occurs due to the transition from a laminar boundary layer in the stagnation region to a turbulent boundary layer in the wall jet region.

Acknowledgement

This work was supported by a grant No. KOSEF 951-1007-007-1 from the Korea Science and Engineering Foundation.

References

[1] H. Martin, Heat and mass transfer between impinging gas jets and solid surfaces, Advances in Heat Transfer, Academic Press, New York, 13 (1977) 1–60.
[2] K. Jambunathan, E. Lai, M.A. Moss, B.L. Button, A review of heat transfer data for single circular jet impingement, Int. J. of Heat and Fluid Flow 13 (2) (1992) 106–115.
[3] R. Viskanta, Heat transfer to impinging isothermal gas and flame jets, Exp. Thermal and Fluid Sci. 6 (1993) 111–134.
[4] R.E. Chupp, H.E. Helms, P.W. McFadden, T.R. Brown, Evaluation of internal heat transfer coefficients for impingement cooled turbine airfoils, J. of Aircraft 6 (1969) 203–208.
[5] H. Thomann, Effect of streamwise wall curvature on heat transfer in a turbulent boundary layer, J. Fluid Mech. 33 (1968) 283–92.
[6] P. Hrycak, Heat transfer and flow characteristics of jets impinging on a concave hemispherical plate, Proc. of Int. Heat Transfer Conf. 3 (1982) 357–362.
[7] C. Gau, C.M. Chung, Surface curvature effect on slot-sir jet impingement cooling flow and heat transfer process, ASME J. of Heat Transfer 113 (1991) 858–864.
[8] G.Y. Yang, M.S. Choi, J.S. Lee, An experimental study of jet impinging cooling on the semi-circular concave surface. Trans. KSME J. 19 (1995) 1083–1094.
[9] D.H. Lee, R. Greif, S.J. Lee, J.H. Lee, Heat transfer from a flat plate to a fully developed axisymmetric impinging jet, ASME J. of Heat Transfer 117 (1995) 772–776.
[10] D.H. Lee, S.J. Lee, J.H. Lee, Heat transfer measurements using liquid crystal with an elliptic jet impinging upon the flat surface, Int. J. of Heat Mass Transfer 37 (1994) 967–976.
[11] J.W. Baughn, P.T. Ireland, T.V. Jones, N. Saniei N, A comparison of the transient and heated-coating methods for the measurements of the local heat transfer coefficients on a pin fin, ASME J. of Heat Transfer 111 (1989) 877–881.
[12] S.J. Kline, F.A. McKlintock, Describing uncertainties in single sample experiments, Mech. Engng 75 (1953) 3–8.
[13] X. Yan, A preheated-wall transient method using liquid crystals for the measurement of heat transfer on external surfaces and in ducts, Ph.D. Dissertation, University of California, Davis, 1993.
[14] K. Kataoka, Optimal nozzle-to-plate spacing for convective heat transfer in non-isothermal, variable density impinging jets, Drying Tech. 3 (1985) 235–254.
[15] D.H. Lee, Y.S. Chung, D.S. Kim, Turbulent flow and heat transfer measurements on a curved surface with a fully developed round impinging jet, Int. J. of Heat and Fluid Flow 18 (1997) 160–169.
[16] B.R. Hollworth, L.R. Gero, Entrainment effects on impingement heat transfer: Part II—local heat transfer measurements, ASME J. of Heat Transfer 107 (1985) 910–915.